

## Field propagator of a dressed junction: Fluorescence lifetime calculations in a confined geometry

Adel Rahmani,\* Patrick C. Chaumet, and Frédérique de Fornel

*Laboratoire de Physique de l'Université de Bourgogne, UPRES A CNRS 5027, Faculté des Sciences Mirande, Boîte Postale 400, 21011 Dijon Cedex, France*

Christian Girard

*Laboratoire de Physique Moléculaire, UMR CNRS 6624, Université de Franche-Comté, 25030 Besançon Cedex, France*

(Received 5 February 1997; revised manuscript received 10 June 1997)

The study of the fluorescence phenomenon by near-field optical techniques requires one to describe precisely the spontaneous emission change occurring when the fluorescing particle is placed in a complex optical environment. For this purpose, the field susceptibility (also called the field propagator) of a planar junction formed by a cavity bounded by two semi-infinite bodies with arbitrary optical constant is derived within the framework of linear-response theory. The field propagator associated with the junction is then modified in a self-consistent manner to account for the presence of any arbitrary object inside the junction. As a first illustration the alteration of the fluorescence lifetime of a molecule by two subwavelength-sized dielectric spheres, placed inside the junction, is presented. [S1050-2947(97)06710-3]

PACS number(s): 42.50.Ct, 32.70.Cs, 32.70.Jz, 07.79.Fc

### I. INTRODUCTION

The interaction of electromagnetic radiation with matter is a cornerstone of modern physics, and a considerable body of literature exists on the subject. Generally, the way of addressing a problem in which an atom or a molecule couples to the electromagnetic field (EMF) is not unique. The choice of an adequate formalism depends on the nature of the material system, and on which aspect of the interaction is to be studied. When the interaction takes place in free space several approaches, both classical and quantum mechanical, exist where expressions for the EMF stem from Maxwell's equations in free space [1–4]. On the other hand, the development of near-field optics (NFO) entailed an increasing demand for theoretical approaches in which the effect of arbitrary geometries on the EMF is accounted for [5]. A description of the interaction of the EMF with matter in terms of field susceptibility is extremely fruitful, since the field susceptibility not only accounts for the field changes induced by a point source but also relates to fundamental quantities such as level shifts, transition rates, and dispersion energies [6,7]. Until recently theoretical works able to couple microscopic compounds (atoms or molecules) with the experimental configurations used in scanning near-field microscopy (SNOM) had been scarce because of the difficulty of matching the boundary conditions for the EMF in an arbitrary geometry [8–10]. As described in Ref. [11], these usual difficulties can be overcome, for instance, by solving the Dyson equation associated with the surroundings of the fluorescing particle, from a pure self-consistent numerical procedure. Another alternative consists in discretizing the entire surface of the object by a dipolar distribution. The response field lying outside the object is then expanded by applying

dipolar solutions that fulfill the boundary conditions [12]. In the efficient approach described in Ref. [11], the numerical iterative scheme begins from a knowledge of the vacuum field susceptibility. Nevertheless, as already proposed in a recent study devoted to electrostatic field computations [13], in order to schematize the complete dielectric surroundings properly, it is more realistic to start the calculation with the retarded field susceptibility of a less symmetrical system. In that case, the field susceptibility associated with two surfaces composing a plane cavity is a prerequisite of any calculation involving more complex structures. However, in Ref. [13] the calculations did not account for retardation effects. When the atom is located in the vicinity of a single plane interface (or more generally a layered half-space) several theoretical approaches (based on different representations of the EMF) have been proposed [14–21]. The framework of some of these theories has been enlarged to allow a second semi-infinite body to be introduced [6,22–26]. Related works dealing with other geometries were reported in Ref. [27]. It is worth noting that in all these works (excepting the second paper in Ref. [21]), it was assumed that either there was a single particle or in the case where more than one particle were considered that there was no interaction between them. With these assumptions, all that was needed was the electric field at the location of the particle. This was possible because the interfaces around the particle were supposed to be free. Nevertheless, if more than one particle (or any polarizable object) is inside the cavity, the knowledge of the field everywhere in the cavity becomes essential since all the objects are coupled to each other. Therefore the purpose of the present work is twofold. First, we derive the field susceptibility of a realistic junction formed by a cavity bounded by two media with arbitrary optical constants. This first step consists of finding the response field of the bare junction to a fluctuating dipole moment. From this response function it will be possible to explore the fluorescence lifetime changes with respect to the position of the particle inside the cavity.

\*Electronic address: arahmani@u-bourgogne.fr

In a second step, we will account for the presence of other additional objects inside the junction by dressing, in a self-consistent manner, the propagator of the bare junction. To the best of our knowledge, such a calculation including retardation effects and based on the concept of dressed junction is not yet available in the literature. The organization of the paper is as follows. In Sec. II we first recall some basic notions of linear response theory merely to relate lifetime and field susceptibility. Physical considerations show that a fully quantum-mechanical description of the interaction can be achieved through classical calculations. Once this is pointed out, we derive the field susceptibility of a junction by calculating the EMF, due to a dipolar source, located at an arbitrary position inside the cavity. For computational purposes, we split the propagator into two contributions, associated with propagating waves and evanescent ones. In order to lend credence to our calculation we study, in Sec. III, the modifications of spontaneous emission for an atom or a molecule placed inside the junction. Starting from the field-susceptibility propagator of the bare junction, we consider, in Sec. IV, the problem of the presence inside the junction of an object with arbitrary shape and nature. We show how a dressed propagator accounting for the presence of the object can be derived self-consistently from the knowledge of the “bare propagator.” As a first study we compute the field propagator of two subwavelength-sized dielectric spheres, and this new propagator is finally used to illustrate how a fluorescing particle can act as a near-field probe.

## II. FIELD SUSCEPTIBILITY

### A. Linear-response theory

Before dealing with the problem of the susceptibility tensor of the junction we might briefly recall some basic results of linear-response theory [28,29]. When the field can be considered as a reservoir (this is particularly the case with a field in thermal equilibrium) and when the calculation is performed up to second order in the interaction Hamiltonian, the interaction between radiation and an atomic system can be described by statistical quantities. Let us consider an atom located at  $\mathbf{r}_0$  in an infinite medium. The only assumption we make on the field is that it should be *stationary*, i.e., the character of the fluctuations of the field does not change with time. We assume the interaction between radiation and the atom to take the form

$$H_{int} = -\mathbf{F} \cdot \mathbf{A}, \quad (1)$$

where  $\mathbf{F}$  ( $\mathbf{A}$ ) is an hermitian observable associated with the field (atomic system). The (free-space) linear susceptibility of the field, that is, the (average) response of the field to a small excitation is given by

$$\hat{\mathbf{S}}_0(\mathbf{r}, \mathbf{r}', \tau) = \frac{i}{\hbar} \langle [\mathbf{F}(\mathbf{r}, t), \mathbf{F}(\mathbf{r}', t - \tau)]_F \Theta(\tau) \rangle. \quad (2)$$

The brackets denote an average over the initial state of the field (as if the atom were not present), and  $\Theta(\tau)$  is the Heaviside step function. In the problem we are investigating in this paper, namely the modification of fluorescence properties by NFO architectures, the level energy shifts are negligible. Therefore, we shall only be interested in the transition rate at

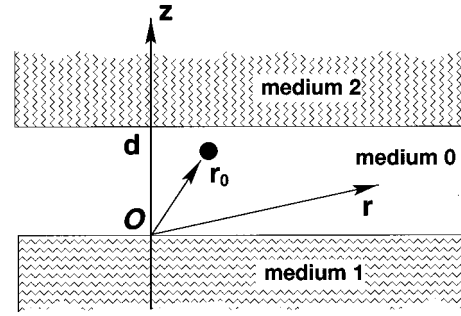


FIG. 1. Geometry of the junction. The particle is located at  $\mathbf{r}_0$ .

which the quantum system (for which we adopt the two-level model) changes its state from an *excited* ( $b$ ) to a *ground* ( $a$ ) state. This rate, given by Fermi's golden rule, reads

$$\Gamma_{0_{ba}} = \frac{2}{\hbar} \sum_{\alpha, \beta} \mu_{\alpha}^{ab} \mu_{\beta}^{ba} \text{Im}[S_{0_{\alpha\beta}}(\mathbf{r}_0, \mathbf{r}_0, \omega)] \quad (3)$$

where  $\mathbf{S}_0(\mathbf{r}, \mathbf{r}', \omega)$  is the Fourier transform of  $\hat{\mathbf{S}}_0(\mathbf{r}, \mathbf{r}', \tau)$ . We have noted  $\mu^{ab}$  the off-diagonal element of the dipole moment operator  $\boldsymbol{\mu}$  between the states  $a$  and  $b$ .  $\text{Im}(X)$  denotes the imaginary part of  $X$ . In view of the results for the free-space field susceptibility, we guess that we should proceed along the preceding lines with the replacement  $\mathbf{S}_0 \rightarrow \mathbf{S}_0 + \mathbf{S}$  in order to find levels shifts and transition rates in the junction. However, as it is correct to think that all that is needed is the susceptibility of the junction ( $\mathbf{S}$ ), it remains to find how to calculate it quantum mechanically. Indeed, if we look at Eq. (2) we might think that we first have to derive the field (the electric field, for instance) operator that intervenes in the interaction Hamiltonian, and then calculate its two-space-time commutator to obtain the end  $\mathbf{S}(\mathbf{r}, \mathbf{r}', \omega)$ . Such a procedure assumes field quantization, which we wish to avoid. The solution lies in the physical nature of the field susceptibility. The field susceptibility is a classical quantity [2,28], and the way the calculation is done—by considering classical or quantum mechanical sources—has no consequence on the consistency of the result with respect to quantum mechanics.

### B. Source and response fields in a bare junction

In order to derive the field susceptibility that accounts for the presence of media 1 and 2, we consider a classical oscillating dipole placed within the junction (Fig. 1). The calculation of the fields in the junction follows that by Agarwal [6], and here we will only give the main steps.

From Maxwell's equation in vacuum we can deduce both the source and the response fields in the cavity:

$$\nabla^2 \mathbf{E} + k_0^2 \mathbf{E} = -4\pi [k_0^2 \mathcal{P} + \nabla(\nabla \cdot \mathcal{P})], \quad (4)$$

$$\mathbf{H} = \nabla \times \mathbf{E} / ik_0, \quad (5)$$

with  $k_0 = \omega/c$  and the polarization  $\mathcal{P}(\mathbf{r}, \omega) = \mathbf{p}(\omega) \delta(\mathbf{r} - \mathbf{r}_0)$  in our case. On the other hand, the fields in medium  $i$  ( $i = 1$  or  $2$ ) obey the following homogeneous equations:

$$\nabla^2 \mathbf{E} + k_0^2 \epsilon_i \mathbf{E} = \mathbf{0}, \quad (6)$$

$$\nabla \cdot \mathbf{E} = 0, \quad (7)$$

$$\mathbf{H} = \nabla \times \mathbf{E} / ik_0. \quad (8)$$

On using an angular spectrum representation [4] of the fields in the cavity, we obtain

$$\mathbf{E}^{(1)}(\mathbf{r}, \omega) = \iint \mathcal{E}^{(1)}(k_x, k_y, \omega) \exp[i\mathbf{K}_1 \cdot \mathbf{r}] dk_x dk_y, \quad (9)$$

$$\mathbf{K}_1 \cdot \mathcal{E}^{(1)} = 0, \quad (10)$$

$$\mathbf{K}_1 = (k_x, k_y, -w_1), \quad w_1^2 = \epsilon_1 k_0^2 - k_x^2 - k_y^2 \quad (11)$$

for medium 1,

$$\mathbf{E}^{(2)}(\mathbf{r}, \omega) = \iint \mathcal{E}^{(2)}(k_x, k_y, \omega) \exp[i\mathbf{K}_2 \cdot \mathbf{r}] dk_x dk_y, \quad (12)$$

$$\mathbf{K}_2 \cdot \mathcal{E}^{(2)} = 0, \quad (13)$$

$$\mathbf{K}_2 = (k_x, k_y, w_2), \quad w_2^2 = \epsilon_2 k_0^2 - k_x^2 - k_y^2 \quad (14)$$

for medium 2, and

$$\begin{aligned} \mathbf{E}^{(0)}(\mathbf{r}, \omega) &= \iint \mathcal{E}^{(+)}(k_x, k_y, \omega) \exp[i\mathbf{K}_0 \cdot \mathbf{r}] \\ &+ \mathcal{E}^{(-)}(k_x, k_y, \omega) \exp[i\mathbf{K}'_0 \cdot \mathbf{r}] dk_x dk_y + \frac{i}{2\pi} \\ &\times \iint \frac{dk_x dk_y}{w_0} [k_0^2 \mathbf{p} + \nabla(\mathbf{p} \cdot \nabla)] \exp[ik_x(x-x_0) \\ &+ ik_y(y-y_0) + iw_0|z-z_0|], \end{aligned} \quad (15)$$

and

$$\mathbf{K}_0 \cdot \mathcal{E}^{(+)} = 0, \quad \mathbf{K}'_0 \cdot \mathcal{E}^{(-)} = 0, \quad \mathbf{K}_0 = (k_x, k_y, w_0),$$

$$\mathbf{K}'_0 = (k_x, k_y, -w_0), \quad w_0^2 = k_0^2 - k_x^2 - k_y^2 \quad (16)$$

for medium 0.

As it can be seen, the field inside the cavity is treated at once rather than considering the infinite sum of the modes undergoing multiple reflection at the interfaces. The last term in Eq. (15) represents the source term, and is put into this form with the help of Weyl's transformation [4]. Expressing the boundary conditions for the electric and magnetic fields at the two interfaces ( $z=0$  and  $z=d$  of the junction), after some straightforward though tedious calculations we obtain a relation between the angular plane-wave amplitudes ( $\mathcal{E}^{(i)}$ ,  $i=1,2,\pm$ ) and the dipole moment [6]. For our present purpose we only need the field inside the cavity from which the field susceptibility can be put in form

$$\begin{aligned} \mathbf{S}(\mathbf{r}, \mathbf{r}_0, \omega) &= \frac{i}{2\pi} \iint [\mathbf{G}^{(+)}(k_x, k_y) \exp(i\mathbf{K}_0 \cdot \mathbf{r}) \\ &+ \mathbf{G}^{(-)}(k_x, k_y) \exp(i\mathbf{K}'_0 \cdot \mathbf{r})] dk_x dk_y. \end{aligned} \quad (17)$$

The tensors  $\mathbf{G}^{(+)}(k_x, k_y)$  (respectively,  $\mathbf{G}^{(-)}(k_x, k_y)$ ) can be viewed as the *elementary* field susceptibility which gives the contribution of the dipole to the  $\mathcal{E}^{(+)}$  upward (respectively,  $\mathcal{E}^{(-)}$  downward) mode of the angular spectrum characterized by  $(k_x, k_y)$ , i.e., we have

$$\mathcal{E}^{(\pm)} = \mathbf{G}^{(\pm)} \cdot \boldsymbol{\mu}. \quad (18)$$

The elements of the  $\mathbf{G}$  tensors are given in Appendix A.

### C. Analytical form of the field

In the following we derive in some detail the  $S_{zz}$  element of the field susceptibility; the other elements stem from a similar algebra, and only the final result is given in Appendix B. Let  $\Delta_{s1}$  and  $\Delta_{p1}$  be the Fresnel reflection coefficient for  $s$  (electric field perpendicular to the plane of incidence) and  $p$ -polarized (electric field parallel to the plane of incidence) plane or evanescent waves falling onto the interface between medium 0 and medium 1. Similarly we define  $\Delta_{s2}$  and  $\Delta_{p2}$  for the  $z=d$  interface:

$$\begin{aligned} \Delta_{p1} &= \frac{w_1 - \epsilon_1 w_0}{w_1 + \epsilon_1 w_0}, \quad \Delta_{p2} = \frac{w_2 - \epsilon_2 w_0}{w_2 + \epsilon_2 w_0}, \\ \Delta_{s1} &= \frac{w_1 - w_0}{w_1 + w_0}, \quad \Delta_{s2} = \frac{w_2 - w_0}{w_2 + w_0}. \end{aligned} \quad (19)$$

The modulus  $k_0$  of the wave vector in medium 0 is given by  $k_0^2 = k_{\parallel}^2 + w_0^2$  ( $k_{\parallel}$  being the component parallel to the interfaces). For the  $zz$  element of the spectrum mode susceptibility we have, from Eqs. (A16) and (A25),

$$G_{zz}^+ = -\frac{k_{\parallel}^2}{w_0} D_p^{-1} \left[ \exp(-i\mathbf{K}_0 \cdot \mathbf{r}_0) - \frac{\exp(-i\mathbf{K}'_0 \cdot \mathbf{r}_0 - 2iw_0 d)}{\Delta_{p2}} \right] \quad (20)$$

$$G_{zz}^- = \frac{k_{\parallel}^2}{w_0} D_p^{-1} \left[ \frac{\exp(-i\mathbf{K}_0 \cdot \mathbf{r}_0)}{\Delta_{p1}} - \exp(-i\mathbf{K}'_0 \cdot \mathbf{r}_0) \right]. \quad (21)$$

If we replace Eqs. (20) and (21) in Eq. (17), we find

$$\begin{aligned} S_{zz}(\mathbf{r}, \mathbf{r}_0, \omega) &= \frac{i}{2\pi} \int d\mathbf{k}_{\parallel} \frac{k_{\parallel}^2 D_p^{-1}}{w_0} \left\{ e^{iw_0(z-z_0)} + e^{-iw_0(z-z_0)} \right. \\ &\quad \left. - \frac{e^{iw_0(z+z_0-2d)}}{\Delta_{p2}} - \frac{e^{-iw_0(z+z_0)}}{\Delta_{p1}} \right\} \\ &\quad \times \exp[i\mathbf{k}_{\parallel} \cdot (\mathbf{r} - \mathbf{r}_0)]. \end{aligned} \quad (22)$$

Since the junction is invariant under rotation about the  $z$  axis, we will work with polar coordinates rather than Cartesian coordinates. Replacing  $d\mathbf{k}_{\parallel}$  by  $k_{\parallel} dk_{\parallel} d\theta$ ,  $D_p^{-1}$  by its value (A7) and performing the angular integration introduces the zeroth-order Bessel function of the first kind, so as to yield [30]

$$\begin{aligned}
S_{zz}(\mathbf{r}, \mathbf{r}_0, \omega) &= i \int_0^{+\infty} dk_{\parallel} \frac{k_{\parallel}^3}{w_0} \frac{J_0(k_{\parallel} R)}{\Delta_{p1} \Delta_{p2} - e^{-2iw_0 d}} \\
&\times \{ e^{iw_0(z+z_0-2d)} \Delta_{p1} + e^{-iw_0(z+z_0)} \Delta_{p2} \\
&- \Delta_{p1} \Delta_{p2} (e^{iw_0(z-z_0)} + e^{-iw_0(z-z_0)}) \}, \quad (23) \\
R &= \sqrt{(x-x_0)^2 + (y-y_0)^2}.
\end{aligned}$$

Further simplification can be gained by integrating Eq. (23) over the *normal* component of the wave vector, leading to

$$\begin{aligned}
S_{zz}(\mathbf{r}, \mathbf{r}_0, \omega) &= i \left( \int_0^{k_0} - \int_0^{i\infty} \right) dw_0 \\
&\times \frac{(k_0^2 - w_0^2) J_0(R \sqrt{k_0^2 - w_0^2})}{\Delta_{p1} \Delta_{p2} - e^{-2iw_0 d}} \\
&\times \{ e^{iw_0(z+z_0-2d)} \Delta_{p1} + e^{-iw_0(z+z_0)} \Delta_{p2} \\
&- \Delta_{p1} \Delta_{p2} (e^{iw_0(z-z_0)} + e^{-iw_0(z-z_0)}) \}. \quad (24)
\end{aligned}$$

Equation (24) is our final result for  $S_{zz}$ . We see that the radiative and nonradiative contributions to the field susceptibility come out naturally. The first integral extends over the *propagating* modes of the field, while the second one obviously involves imaginary values of the normal component of the wave vector and hence relates to *evanescent* modes. Chance, Prock, and Silbey (CPS) discussed a similar separation for the case  $R=0$ , although their calculation was based on a different method [24]. They used a representation of the electromagnetic field based on the Hertz potential vector in an approach similar to Sommerfeld's treatment of radio-wave propagation above the earth [31]. In their work, the separation between radiative and nonradiative decay rates was achieved by computing the flow of electromagnetic energy (Poynting's vector) through planes placed below and above the dipole. The other elements of the field susceptibility stem from similar algebra. Further simplification of Eq. (24) will depend on the exact nature of the media 1 and 2 involved. In the case where one of the media recedes to infinity, one might check that the field susceptibility of a single surface is recovered. Now that we have derived the field susceptibility, we consider, in Sec. III, the case of a particle (atom or molecule) placed inside the junction for which we study the evolution of the lifetime.

### III. LIFETIME MODIFICATION

In this section we treat the particle as a *classical* oscillating dipole whose oscillations are inhibited or enhanced by the electric field at its location. The equation of motion for such a dipole reads

$$\ddot{\mu} + \Gamma \dot{\mu} + \omega^2 \mu = \frac{e^2}{m} E_{\text{junct}}. \quad (25)$$

$E_{\text{junct}}$  is the projection along the dipole direction of the response field of the junction at the particle's location, and  $\Gamma$  is a phenomenological damping coefficient we shall formally

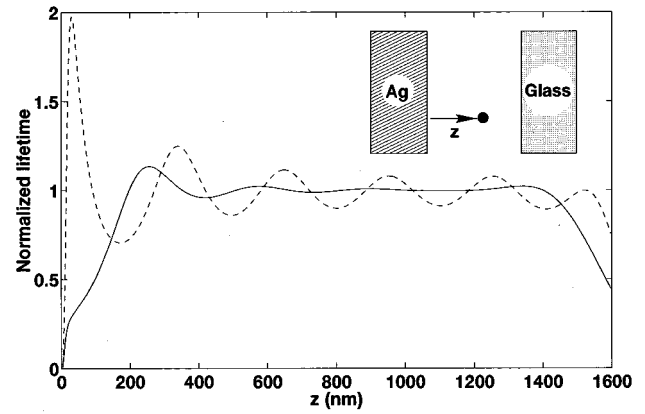


FIG. 2. Normalized lifetime as a function of the position of the atom inside a junction between silver and glass ( $\epsilon=2.25$ ). The height of the cavity is 1600 nm. Solid line: perpendicular dipole; dashed line: parallel dipole. Except when indicated otherwise, the normalization is done with respect to an atom in free space.

identify with the quantum mechanical transition rate (the lifetime is given by  $\tau=1/\Gamma$ ). If the solutions are sought in the form  $A_0 \exp[-i\Omega t]$  with  $\Omega$  complex, the damping rate is found by identifying from Eq. (25) the imaginary part of  $\Omega$ . The lifetime of the atom (normalized with respect to the free space value) is given by [24,27]

$$\frac{\tau}{\tau_0} = \frac{\Gamma_0}{\Gamma} = \left[ 1 + \frac{3}{2} \text{Im} \left( \frac{c^3 E_{0\text{junct}}}{n_0 \omega^3 \mu_0} \right) \right]^{-1}. \quad (26)$$

If we assume that medium 0 is air ( $n_0=1$ ), and introduce  $k_0=\omega/c$  and the field susceptibility, we find, in the case of a dipole aligned with the  $z$  axis,

$$\left( \frac{\tau}{\tau_0} \right)_z = \left[ 1 + \frac{3}{2} \text{Im} \left( \frac{S_{zz}(\mathbf{r}_0, \mathbf{r}_0, \omega)}{k_0^3} \right) \right]^{-1}. \quad (27)$$

It might be worth noting that in this classical picture, the fluorescing particle is seen as an oscillator damped by its coupling with the field, leading to an irreversible decay with a characteristic time  $\tau$  we call the lifetime (this is related to the fact that the coupling between the particle and the field is weak; on the other hand, had this coupling been strong our perturbative approach, based on Fermi's golden rule, would have failed). The correspondence between "this lifetime" and the one given by quantum mechanics will be discussed at the end of this section.

We now turn back to our dipole placed inside the junction. In the following we consider only dipoles parallel and perpendicular to the  $z$  axis for any other orientation can be derived from a combination of these two. The emission wavelength ( $2\pi/k_0$ ) is chosen to be 612 nm. In Fig. 2 we plot the normalized lifetime of an atom as a function of its position in the junction. The cavity height is 1600 nm, and unless it is indicated otherwise all the optical constants for the metals are taken from Ref. [32]. In the middle of the cavity, far from the interfaces, we observe the well-known oscillations in the lifetime due to the interaction with the long-range *propagating* field reflected by the junction. Typical near-field effects, involving *evanescent* modes of the

field, can be observed for shorter distances (subwavelength range from the interfaces). Since in this section we consider a single particle inside the cavity, a direct comparison with the work of CPS is possible. Let us consider a dipole lying along the  $z$  axis located at  $(0,0,z_0)$  in the junction. According to the CPS theory [Eqs. (2.47) and (2.48) of Ref. [24]] and if we adopt the notation of the present paper, the normalized decay rate is

$$\left(\frac{\Gamma}{\Gamma_0}\right)_z = \frac{3}{2} \operatorname{Im} \frac{i}{k_0^3} \left( \int_{k_0}^0 + \int_0^{i\infty} \right) dw_0 (k_0^2 - w_0^2) \times \frac{\Delta_{p1} e^{2iw_0 z_0} + \Delta_{p2} e^{2iw_0(d-z_0)} - 1 - \Delta_{p1} \Delta_{p2} e^{2iw_0 d}}{1 - \Delta_{p1} \Delta_{p2} e^{2iw_0 d}}. \quad (28)$$

On the other hand, on using Eqs. (24) and (27), our calculation leads to

$$\left(\frac{\Gamma}{\Gamma_0}\right)_z = 1 + \frac{3}{2} \operatorname{Im} \frac{i}{k_0^3} \left( \int_{k_0}^0 + \int_0^{i\infty} \right) dw_0 (k_0^2 - w_0^2) \times \frac{\Delta_{p1} e^{2iw_0 z_0} + \Delta_{p2} e^{2iw_0(d-z_0)} - 2\Delta_{p1} \Delta_{p2} e^{2iw_0 d}}{1 - \Delta_{p1} \Delta_{p2} e^{2iw_0 d}}. \quad (29)$$

This last form is also the one given by the Green's-function method described in [24] [Eqs. (3.37) and (3.38)]. With little algebra it is straightforward to show that the two results are identical [34]. Hence the case  $R=0$  of our field propagator leads to the CPS theory for lifetime modification in a three-media junction. Here we will not comment further upon these curves for the physical effects involved (particularly the excitation of plasmon resonance in metals) have been extensively discussed in the literature [33]. In near-field optics experiments, the fluorescent particles are generally adsorbed on a substrate and a probe tip which can either be totally dielectric or covered with metal is brought into the near field of the particle. The actual shape of the tip plays a role in its interaction with the particle, but a qualitative picture of the influence of the material placed above the particle can be obtained with this model of the junction. We consider a fluorescing molecule placed on a glass surface with refractive index  $n=1.5$  ( $\epsilon_1=2.25$ ). When the gap distance  $d$  between media 1 and 2 is reduced, the EMF reflected by the junction at the molecule's position changes and so does the fluorescence lifetime. The cases of a dielectric medium 1 and a dielectric or metallic medium 2 are shown in Fig. 3. The observed behavior as the metallic medium [aluminum in Fig. 3(a)] is brought close to the fluorescing molecule strongly resembles that observed in Fig. 2. We find again the standard features already described: far-field induced oscillations, lifetime enhancement, and decrease as the metal reaches the fluorescing particle. The influence of the substrate consists merely in renormalizing the lifetime with respect to the free-space value leading, for large separations between the particle and medium 2, to the values for a vacuum-glass interface [34].

The dielectric case described in Fig. 3(b) might deserve further attention. When both media 1 and 2 have the same

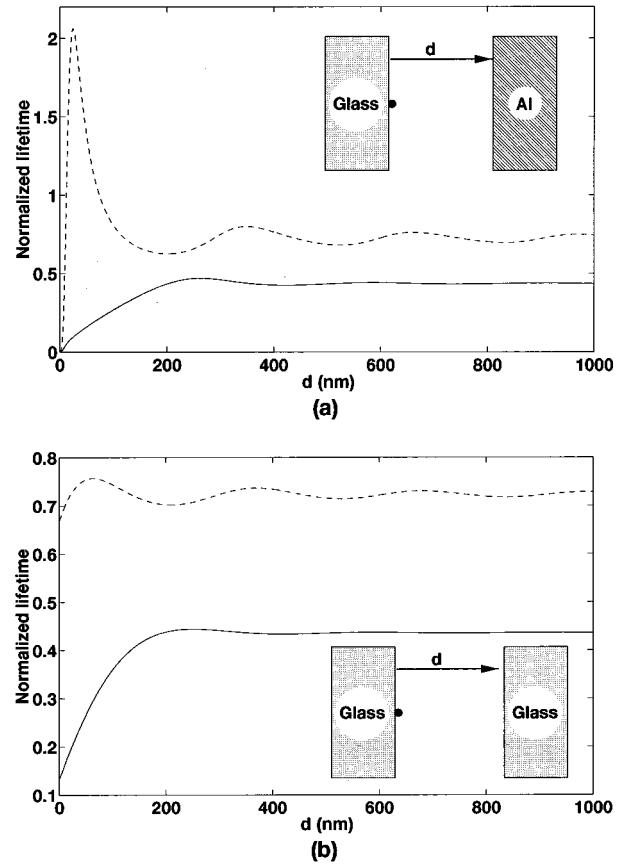


FIG. 3. Normalized lifetime for a dipole on a glass substrate as a function of the gap height. Medium 2 is (a) aluminum, (b) glass; solid line: perpendicular dipole; dashed line: parallel dipole.

refractive index ( $n_1=1.5$ ), as the gap is shortened the junction tends toward a bulk and homogeneous medium with (real) index  $n_1$ . In such a homogeneous medium we know that the fluorescence lifetime of the molecule should be  $\tau_0/n_1$ . Actually, this value is indeed the ultimate value for the parallel dipole as  $d$  goes to zero, but the lifetime for the perpendicular dipole obviously tends toward a much smaller value ( $\tau_0/n_1^5$ ). To reconcile these two remarks let us consider a dipole parallel to the interfaces. As the gap between media 1 and 2 decreases, the electric field emitted by the dipole and arriving at the interfaces 0/1 and 0/2 becomes purely *tangential*. Therefore it is continuous across the interfaces ( $E_1=E_0$  for the 0/1 interface). Conversely, in the case of dipole perpendicular to the interfaces, for small values of  $d$  the electric field generated at the interfaces is purely *normal* and thus we have  $\epsilon_0 E_0 = \epsilon_1 E_1$ . The normalized decay rate  $\Gamma'$  in an infinite medium 1 represents the normalized power emitted by the dipole and it is proportional to the square of  $E_1$  at the dipole's location  $\mathbf{r}_0$ . In the case of a dipole in a thin layer (medium 0 in the limit  $d \rightarrow 0$ ), the field at  $\mathbf{r}_0$  is given by  $E_0(\mathbf{r}_0) = E_1(\mathbf{r}_0)$  and  $E_0(\mathbf{r}_0) = \epsilon_1 E_1(\mathbf{r}_0)$  for a parallel and a perpendicular dipole, respectively (we take  $\epsilon_0=1$ ). Therefore the decay rate ( $\Gamma$ ), for the dipole in medium 0, equals  $\Gamma'$  for a parallel dipole and  $\epsilon_1^2 \Gamma'$  ( $=n_1^4 \Gamma'$ ) for a perpendicular dipole. Once we replace  $\Gamma'$  by its value  $n_1 \Gamma_0$  the correct limiting values for the lifetime ( $\tau/\tau_0 = \Gamma_0/\Gamma$ ) are found. The reader interested in a different but more formal derivation of this property is referred to Ref. [25].

We might note for completeness that since all the relevant information concerning the interfaces are contained in the Fresnel coefficients, the case of a stratified environment can be addressed through the replacement of the Fresnel coefficients (19) by the ones relative to a multilayer system [18,25]. Before addressing the problem of many-body interaction inside the junction we return to the question of whether the assumption that the atom or the molecule can be seen as a classical dipole is appropriate when calculating the lifetime changes.

In Sec. II, we mentioned the fact that the field susceptibility is a classical quantity. Therefore we understand that the classical calculation of Sec. III gives a field susceptibility valid in a quantum approach. However, the curves presented in the last paragraph were obtained with a classical expression for the lifetime and not from Eq. (3). We might briefly check that the transition rate given by Fermi's golden rule leads exactly to Eq. (27) for the normalized lifetime. From Eq. (3) we infer that

$$\Gamma_{0_{ba}} = \frac{2}{\hbar} \sum_{\alpha,\beta} \mu_{\alpha}^{ab} \mu_{\beta}^{ba} \text{Im}[S_{0_{\alpha\beta}}(\mathbf{r}_0, \mathbf{r}_0, \omega)] \quad (30)$$

for the decay rate in free space, and

$$\Gamma_{ba} = \frac{2}{\hbar} \sum_{\alpha,\beta} \mu_{\alpha}^{ab} \mu_{\beta}^{ba} \text{Im}[S_{0_{\alpha\beta}}(\mathbf{r}_0, \mathbf{r}_0, \omega) + S_{\alpha\beta}(\mathbf{r}_0, \mathbf{r}_0, \omega)] \quad (31)$$

for the decay rate in the junction. Since we are interested in normalized values, we write

$$\frac{\Gamma_{ba}}{\Gamma_{0_{ba}}} = 1 + \frac{2}{\hbar \Gamma_{0_{ba}}} \sum_{\alpha,\beta} \mu_{\alpha}^{ab} \mu_{\beta}^{ba} \text{Im}[S_{\alpha\beta}(\mathbf{r}_0, \mathbf{r}_0, \omega)]. \quad (32)$$

If we now replace  $\Gamma_{0_{ba}}$  by the common value for the decay of an atom in free space [35],

$$\frac{4k_0^3}{3\hbar} |\boldsymbol{\mu}^{ba}|^2, \quad (33)$$

and take the reciprocal of Eq. (32), we recover, in the case of a dipole moment aligned along the  $z$  axis, the result given by Eq. (27). This correspondence between the classical and the quantum-mechanical results arises from the fact that the boundaries (media 1 and 2) modify in the same way the effect on the particle of radiation reaction and of vacuum fluctuations [36].

#### IV. FIELD PROPAGATOR OF A DRESSED JUNCTION

The relation between the field susceptibility and the lifetime of an atom or a molecule placed inside a planar junction was discussed in Sec. III. However, if we introduce any object inside the junction the field susceptibility will be modified, and will differ significantly from that associated with a simple bare junction. Actually, it is possible to build the field susceptibility tensor of an arbitrary system by solving a sequence of Dyson's equations [37]. For instance let us consider a small polarizable object located at  $\mathbf{r}_s = (x_s, y_s, z_s)$  in medium 0, and its dynamical polarizability is noted  $\boldsymbol{\alpha}(\omega)$ .

The resulting (dressed) field susceptibility  $\mathbf{S}_D$  verifies the following self-consistent equation:

$$\mathbf{S}_D(\mathbf{r}', \mathbf{r}, \omega) = \mathbf{S}_0(\mathbf{r}', \mathbf{r}, \omega) + \mathbf{S}(\mathbf{r}', \mathbf{r}, \omega) + [\mathbf{S}_0(\mathbf{r}', \mathbf{r}_s, \omega) + \mathbf{S}(\mathbf{r}', \mathbf{r}_s, \omega)] \cdot \boldsymbol{\alpha}(\omega) \cdot \mathbf{S}_D(\mathbf{r}_s, \mathbf{r}, \omega), \quad (34)$$

where the tensor  $\mathbf{S}_0$  is the (three dimensional) field susceptibility in free space [1].

For lifetime calculations, the knowledge of  $\mathbf{S}_D$  at the molecule's location ( $\mathbf{r}_0$ ) is necessary. In that case we write

$$\mathbf{S}_D(\mathbf{r}_0, \mathbf{r}_0, \omega) = \mathbf{S}(\mathbf{r}_0, \mathbf{r}_0, \omega) + [\mathbf{S}_0(\mathbf{r}_0, \mathbf{r}_s, \omega) + \mathbf{S}(\mathbf{r}_0, \mathbf{r}_s, \omega)] \cdot \boldsymbol{\alpha}(\omega) \cdot \mathbf{S}_D(\mathbf{r}_s, \mathbf{r}_0, \omega), \quad (35)$$

where  $\mathbf{S}_D(\mathbf{r}_s, \mathbf{r}_0, \omega)$  can be deduced by solving Eq. (34). If an additional object is inserted, we proceed along the preceding lines with the replacement  $\mathbf{S}(\mathbf{r}', \mathbf{r}, \omega) \rightarrow \mathbf{S}_D(\mathbf{r}', \mathbf{r}, \omega)$ . Hence, for an arbitrary object, with a dielectric function  $\epsilon(\omega)$ , a discretization procedure makes it possible to construct the field susceptibility of the dressed junction "piece by piece." The object is thus considered as a collection of  $N$  polarizable units (dipoles) placed on a (usually) cubic lattice. When the size of the discretization cell (size of one polarizable unit) is much smaller than the wavelength of the incident field, one can use the discrete dipole approximation introduced by Purcell and Pennypacker [38]. Let  $l$  be the size of the discretization cell; the polarizability of a dipolar subunit then reads

$$\boldsymbol{\alpha}(\omega) = \frac{3l^3}{4\pi} \frac{\epsilon(\omega) - 1}{\epsilon(\omega) + 2} \mathbf{I}, \quad (36)$$

where  $\mathbf{I}$  is the unit tensor. We might note that unlike the definition

$\boldsymbol{\alpha}(\omega) = l^3 [\epsilon(\omega) - 1] \mathbf{I} / 4\pi$  used in Refs. [11,37] the present definition of the polarizability includes at once depolarization effects.

An alternate procedure consists in computing the propagators:

$$\mathbf{S}_D(\mathbf{r}_i, \mathbf{r}_0, \omega) = \mathbf{S}_0(\mathbf{r}_i, \mathbf{r}_0, \omega) + \mathbf{S}(\mathbf{r}_i, \mathbf{r}_0, \omega) + \sum_{j=1}^N [\mathbf{S}_0(\mathbf{r}_i, \mathbf{r}_j, \omega) + \mathbf{S}(\mathbf{r}_i, \mathbf{r}_j, \omega)] \cdot \boldsymbol{\alpha}_j(\omega) \cdot \mathbf{S}_D(\mathbf{r}_j, \mathbf{r}_0, \omega) \quad (37)$$

for  $i = 1, N$ . The solution of this set of linear equations is then used to calculate

$$\mathbf{S}_D(\mathbf{r}_0, \mathbf{r}_0, \omega) = \mathbf{S}(\mathbf{r}_0, \mathbf{r}_0, \omega) + \sum_{i=1}^N [\mathbf{S}_0(\mathbf{r}_0, \mathbf{r}_i, \omega) + \mathbf{S}(\mathbf{r}_0, \mathbf{r}_i, \omega)] \cdot \boldsymbol{\alpha}_i(\omega) \cdot \mathbf{S}_D(\mathbf{r}_i, \mathbf{r}_0, \omega). \quad (38)$$

While the two methods give the same result and require the same amount of computer memory, the latter is faster, a feature that must be borne in mind when  $N$ , the number of dipoles inside the junction, becomes large. However, some care must be given to the matrix inversion procedure used to solve Eq. (37).

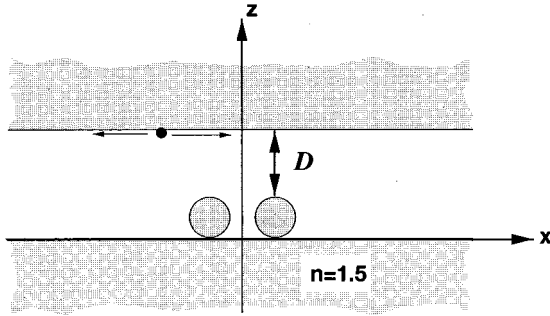


FIG. 4. Geometry of the dressed junction. The sample consists of two spheres with refractive index 1.5 deposited on a substrate (medium 1). Both media 1 and 2 have the same index as the spheres. The diameter of the spheres is 20 nm, and the distance between their centers is 40 nm.

To illustrate this approach let us consider two dielectric spheres, with diameter  $2a = 20$  nm, deposited 20 nm apart on a substrate. The fluorescing molecule is deposited on the second medium. The spheres and both media have the same refractive index ( $n = \sqrt{\epsilon_s} = 1.5$ ). The molecule now plays the role of a nanoprobe used to image a sample (the spheres). The dynamical polarizability of the sphere is given by

$$\alpha(\omega) = a^3 \frac{\epsilon_s(\omega) - 1}{\epsilon_s(\omega) + 2} \mathbf{I}. \quad (39)$$

where  $\mathbf{I}$  is the unit tensor. If we introduce this expression into Eq. (34), we obtain the field susceptibility, which accounts for the presence of the sphere inside the junction (Fig. 4). Each sphere is coupled to the junction through  $\mathbf{S}$  (dressing of the sphere polarizability by the junction) and to the other sphere through  $\mathbf{S}_0$  (direct coupling) and  $\mathbf{S}$  (junction mediated coupling). Similarly, the effect of the spheres on the molecule includes both the direct and cavity-mediated contributions. Although this example might seem far from the situation where the molecule would be attached to a probe with finite lateral dimensions, it includes all the main physical effects. For different values of the distance  $D$  between the molecule (the probe) and the top of the spheres (the sample), in Fig. 5 we have plotted the normalized decay rate (reciprocal of the normalized lifetime) as the molecule scans a  $150 \times 150$ -nm<sup>2</sup> area. When the molecule is scanned at 10 nm [Fig. 5(a)] above the top of the spheres, the modification of the fluorescence is well localized in space, and the influence of the two spheres can be unambiguously separated (the maxima are located 40 nm apart and the width of the peaks is 22-nm full width at half maximum). As the distance of the gap is increased from 10 to 20 [Fig. 5(b)] and ultimately to 40 nm [Fig. 5(c)], the individual contributions are merged, giving a single global bump in the decay rate. If the distance is further increased, the amplitude of the bump will decrease. We recover here a common feature of SNOM, where the near-field nature of the interaction makes it possible to increase the resolution by decreasing the distance between the probe and the sample, without decreasing the wavelength, as is the case in conventional “far-field” optics. However, one must not believe that the gap distance is the only relevant parameter. Indeed when other orientation of the

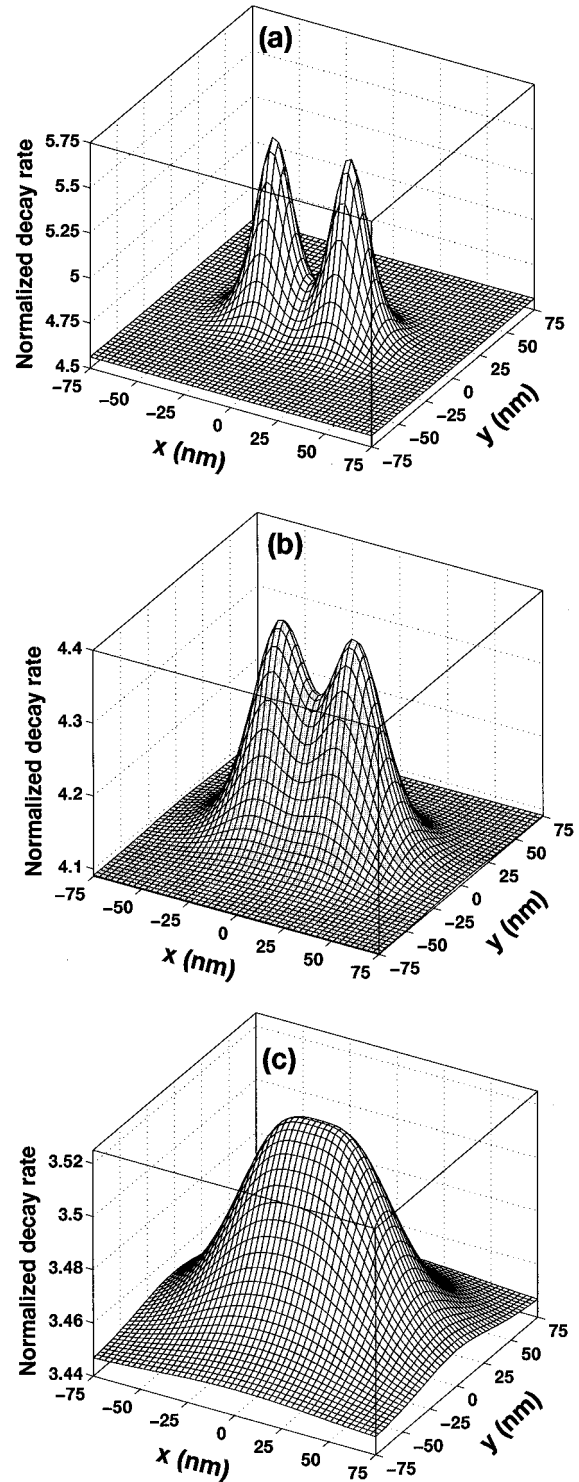


FIG. 5. Three-dimensional plots of the decay rate (normalized with respect to the free space value) as the molecule scans a  $150 \times 150$ -nm<sup>2</sup> area at a distance  $D$  from the top of the spheres. (a)  $D = 10$  nm. (b)  $D = 20$  nm. (c)  $D = 40$  nm.

dipole and/or other nature for the sample (e.g., metallic particles smaller than the wavelength of the fluorescence light) are considered, the observed behavior for the decay rate (or the lifetime) is much more complex and subtle and will not be detailed here.

## V. CONCLUSION

We have used the linear-response theory to derive the field susceptibility of a junction formed by two plane interfaces separating three media with arbitrary optical constant. The validity of such a derivation is justified by the weak interaction between the EMF and the source. This propagator allowed us to describe the modification of spontaneous emission for an atom or a molecule inside the junction. In order to address some nontrivial situations that might be encountered in near-field optics experiments, we have constructed self-consistently a dressed propagator accounting for the presence inside the junction of one or more polarizable objects. Instead of being the sample, the fluorescing particle could then act as a probe illustrating the potential of near-field fluorescence imaging. In the application proposed in this paper, the sample consisted of two dielectric spheres (diameter 20 nm). The fact that the response of each of the two spheres could be separated, at least when the molecule was not too far from them, is a reflection of the confinement of the EMF around them [39]. Thus in confined geometries the gradient of the EMF depends not only on the wavelength but also on the environment. Near objects such as our spheres one should expect a strong gradient of the EMF leading to an increase of the contribution of multipoles higher than the dipole; particularly, in the case where no dipole transition is allowed, a high sensitivity may be achieved by exploiting the quadrupolar transition of the probe particle, as was demonstrated by the recent work of Klimov and Letokhov [40]. On the other hand, this strong gradient of the EMF also suggests some interesting issues related to the forces that might be experienced by the particle. The experimental study of this class of near-field effects presupposes an understanding of the main physical interactions that play a role in a confined geometry. As we have done in this paper, it is always interesting to start with rather simple geometries and then evolve toward more complex ones.

## ACKNOWLEDGMENTS

We would like to thank M. Devel for helpful suggestions concerning the computation of the propagators, and J. P. Dufour for constructive discussions and for his critical reading of the manuscript. We are grateful to W. Jhe for kindly sending us a copy of Ref. [26] prior to publication.

## APPENDIX A: FIELD SUSCEPTIBILITIES OF THE MODES OF THE ANGULAR SPECTRUM

For convenience we introduce the variables

$$A^+ = \exp(-i\mathbf{K}_0 \cdot \mathbf{r}_0) + \frac{\exp(-i\mathbf{K}'_0 \cdot \mathbf{r}_0 - 2iw_0d)}{\Delta_{p2}}, \quad (\text{A1})$$

$$B^+ = \exp(-i\mathbf{K}_0 \cdot \mathbf{r}_0) - \frac{\exp(-i\mathbf{K}'_0 \cdot \mathbf{r}_0 - 2iw_0d)}{\Delta_{s2}}, \quad (\text{A2})$$

$$C^+ = \exp(-i\mathbf{K}_0 \cdot \mathbf{r}_0) - \frac{\exp(-i\mathbf{K}'_0 \cdot \mathbf{r}_0 - 2iw_0d)}{\Delta_{p2}}, \quad (\text{A3})$$

$$A^- = \frac{\exp(-i\mathbf{K}_0 \cdot \mathbf{r}_0)}{\Delta_{p1}} + \exp(-i\mathbf{K}'_0 \cdot \mathbf{r}_0), \quad (\text{A4})$$

$$B^- = \frac{\exp(-i\mathbf{K}_0 \cdot \mathbf{r}_0)}{\Delta_{s1}} - \exp(-i\mathbf{K}'_0 \cdot \mathbf{r}_0), \quad (\text{A5})$$

$$C^- = \frac{\exp(-i\mathbf{K}_0 \cdot \mathbf{r}_0)}{\Delta_{p1}} - \exp(-i\mathbf{K}'_0 \cdot \mathbf{r}_0), \quad (\text{A6})$$

$$D_p = 1 - \frac{\exp(-2iw_0d)}{\Delta_{p1}\Delta_{p2}}, \quad D_s = 1 - \frac{\exp(-2iw_0d)}{\Delta_{s1}\Delta_{s2}}. \quad (\text{A7})$$

### 1. Upward modes: $k_z = w_0$

For the modes whose the  $z$  component of the wave vector is positive, we have

$$G_{xx}^+ = -\frac{w_0 k_x^2}{k_{\parallel}^2} D_p^{-1}[A^+] - \frac{k_y^2 k_0^2}{k_{\parallel}^2 w_0} D_s^{-1}[B^+], \quad (\text{A8})$$

$$G_{xy}^+ = -\frac{w_0 k_x k_y}{k_{\parallel}^2} D_p^{-1}[A^+] + \frac{k_x k_y k_0^2}{k_{\parallel}^2 w_0} D_s^{-1}[B^+], \quad (\text{A9})$$

$$G_{xz}^+ = k_x D_p^{-1}[C^+], \quad (\text{A10})$$

$$G_{yx}^+ = -\frac{w_0 k_x k_y}{k_{\parallel}^2} D_p^{-1}[A^+] + \frac{k_x k_y k_0^2}{k_{\parallel}^2 w_0} D_s^{-1}[B^+], \quad (\text{A11})$$

$$G_{yy}^+ = -\frac{w_0 k_y^2}{k_{\parallel}^2} D_p^{-1}[A^+] - \frac{k_x^2 k_0^2}{k_{\parallel}^2 w_0} D_s^{-1}[B^+], \quad (\text{A12})$$

$$G_{yz}^+ = k_y D_p^{-1}[C^+], \quad (\text{A13})$$

$$G_{zx}^+ = k_x D_p^{-1}[A^+], \quad (\text{A14})$$

$$G_{zy}^+ = k_y D_p^{-1}[A^+], \quad (\text{A15})$$

$$G_{zz}^+ = -\frac{k_{\parallel}^2}{w_0} D_p^{-1}[C^+]. \quad (\text{A16})$$

### 2. Downward modes: $k_z = -w_0$

For the modes whose the  $z$  component of the wave vector is negative, we have

$$G_{xx}^- = -\frac{w_0 k_x^2}{k_{\parallel}^2} D_p^{-1}[A^-] + \frac{k_y^2 k_0^2}{k_{\parallel}^2 w_0} D_s^{-1}[B^-], \quad (\text{A17})$$

$$G_{xy}^- = -\frac{w_0 k_x k_y}{k_{\parallel}^2} D_p^{-1}[A^-] - \frac{k_x k_y k_0^2}{k_{\parallel}^2 w_0} D_s^{-1}[B^-], \quad (\text{A18})$$

$$G_{xz}^- = k_x D_p^{-1}[C^-], \quad (\text{A19})$$

$$G_{yx}^- = -\frac{w_0 k_x k_y}{k_{\parallel}^2} D_p^{-1}[A^-] - \frac{k_x k_y k_0^2}{k_{\parallel}^2 w_0} D_s^{-1}[B^-], \quad (\text{A20})$$



$$G_{yy}^- = -\frac{w_0 k_y^2}{k_{\parallel}^2} D_p^{-1}[A^-] + \frac{k_x^2 k_0^2}{k_{\parallel}^2 w_0} D_s^{-1}[B^-], \quad (\text{A21})$$

$$G_{yz}^- = k_y D_p^{-1}[C^-], \quad (\text{A22})$$

$$G_{zx}^- = -k_x D_p^{-1}[A^-], \quad (\text{A23})$$

$$G_{zy}^- = -k_y D_p^{-1}[A^-], \quad (\text{A24})$$

$$G_{zz}^- = \frac{k_{\parallel}^2}{w_0} D_p^{-1}[C^-]. \quad (\text{A25})$$

### APPENDIX B: FIELD SUSCEPTIBILITY IN THE JUNCTION

As it can be seen in Appendix A, the symmetry of the junction suggests some relations between the elements of the field propagator. Hence five integrals are needed to derive all the elements of the propagator. Let  $\phi$  the angle defined by  $(x-x_0)=R \cos \phi$ , we have

$$\begin{aligned} S_{xx} &= I_1 - I_2 \cos 2\phi, \\ S_{xy} &= S_{yx} = -I_2 \sin 2\phi, \\ S_{xz} &= I_3 \cos \phi, \\ S_{yy} &= I_1 + I_2 \cos 2\phi, \\ S_{yz} &= I_3 \sin \phi, \\ S_{zx} &= I_4 \cos \phi, \\ S_{zy} &= I_4 \sin \phi. \end{aligned} \quad (\text{B1})$$

$S_{zz}$  is calculated directly from Eq. (24).

The integrals of Eq. (B1) are given by

$$\begin{aligned} I_1 &= -\frac{i}{2} \left( \int_0^{k_0} - \int_0^{i\infty} \right) dw_0 J_0(R\sqrt{k_0^2 - w_0^2}) \\ &\times \left\{ \frac{w_0^2}{(\Delta_{p1}\Delta_{p2} - e^{-2iw_0d})} [\Delta_{p1} e^{iw_0(z+z_0-2d)} \right. \end{aligned}$$

$$\begin{aligned} &+ \Delta_{p2} e^{-iw_0(z+z_0)} + \Delta_{p1}\Delta_{p2}(e^{iw_0(z-z_0)} + e^{-iw_0(z-z_0)})] \\ &- \frac{k_0^2}{(\Delta_{s1}\Delta_{s2} - e^{-2iw_0d})} [\Delta_{s1} e^{iw_0(z+z_0-2d)} \\ &+ \Delta_{s2} e^{-iw_0(z+z_0)} - \Delta_{s1}\Delta_{s2}(e^{iw_0(z-z_0)} + e^{-iw_0(z-z_0)})] \left. \right\}, \end{aligned} \quad (\text{B2})$$

$$\begin{aligned} I_2 &= -\frac{i}{2} \left( \int_0^{k_0} - \int_0^{i\infty} \right) dw_0 J_2(R\sqrt{k_0^2 - w_0^2}) \\ &\times \left\{ \frac{w_0^2}{(\Delta_{p1}\Delta_{p2} - e^{-2iw_0d})} [\Delta_{p1} e^{iw_0(z+z_0-2d)} \right. \\ &+ \Delta_{p2} e^{-iw_0(z+z_0)} + \Delta_{p1}\Delta_{p2}(e^{iw_0(z-z_0)} + e^{-iw_0(z-z_0)})] \\ &+ \frac{k_0^2}{(\Delta_{s1}\Delta_{s2} - e^{-2iw_0d})} [\Delta_{s1} e^{iw_0(z+z_0-2d)} \\ &+ \Delta_{s2} e^{-iw_0(z+z_0)} - \Delta_{s1}\Delta_{s2}(e^{iw_0(z-z_0)} + e^{-iw_0(z-z_0)})] \left. \right\}, \end{aligned} \quad (\text{B3})$$

$$\begin{aligned} I_3 &= -\left( \int_0^{k_0} - \int_0^{i\infty} \right) \frac{w_0 \sqrt{k_0^2 - w_0^2}}{(\Delta_{p1}\Delta_{p2} - e^{-2iw_0d})} J_1(R\sqrt{k_0^2 - w_0^2}) \\ &\times \{ \Delta_{p2} e^{-iw_0(z+z_0)} - \Delta_{p1} e^{iw_0(z+z_0-2d)} \\ &+ \Delta_{p1}\Delta_{p2}(e^{iw_0(z-z_0)} - e^{-iw_0(z-z_0)}) \} dw_0, \end{aligned} \quad (\text{B4})$$

$$\begin{aligned} I_4 &= \left( \int_0^{k_0} - \int_0^{i\infty} \right) \frac{w_0 \sqrt{k_0^2 - w_0^2}}{(\Delta_{p1}\Delta_{p2} - e^{-2iw_0d})} J_1(R\sqrt{k_0^2 - w_0^2}) \\ &\times \{ \Delta_{p2} e^{-iw_0(z+z_0)} - \Delta_{p1} e^{iw_0(z+z_0-2d)} \\ &- \Delta_{p1}\Delta_{p2}(e^{iw_0(z-z_0)} - e^{-iw_0(z-z_0)}) \} dw_0. \end{aligned} \quad (\text{B5})$$

The last integral to be calculated is given by Eq. (24).

- 
- [1] J. D. Jackson, *Classical Electrodynamics*, 2nd ed. (Wiley, New York, 1975), p. 395.
- [2] C. Cohen-Tannoudji, J. Dupont-Roc, and G. Grynberg, *Processus d'Interaction Entre Photons et Atomes* (InterEdition, Paris, 1988), complément A<sub>IV</sub>. English translation: *Atom-Photon Interactions: Basic Processes and Applications* (Wiley-Interscience, New York, 1992).
- [3] C. Cohen-Tannoudji, J. Dupont-Roc, and G. Grynberg, *Introduction à l'Électrodynamique Quantique* (InterEdition, Paris, 1987), pp. 223 and 354–358. English translation: *Photons and Atoms: Introduction to Quantum Electrodynamics* (Wiley-Interscience, New York, 1989).
- [4] L. Mandel and E. Wolf, *Optical Coherence and Quantum Op-*

*tics* (Cambridge University Press, Cambridge, 1995), pp. 109–125.

- [5] D. W. Pohl, *Adv. Opt. Electron. Microsc.* **12**, 243 (1991); R. Kopelman, K. Lieberman, A. Lewis, and W. Tan, *J. Lumin.* **48-49**, 871 (1991); E. Betzig and R. J. Chichester, *Science* **262**, 1422 (1993); J. K. Trautman, J. J. Macklin, L. E. Brus, and E. Betzig, *Nature* (London) **369**, 40 (1994); X. S. Xie and R. C. Dunn, *Science* **265**, 361 (1994); W. P. Ambrose, P. M. Goodwin, J. C. Martin, and R. A. Keller, *ibid.* **265**, 364 (1994); A. Jalocha and N. F. van Hulst, *Opt. Commun.* **119**, 17 (1995); T. Saiki, M. Ohtsu, K. Jang, and W. Jhe, *Opt. Lett.* **21**, 674 (1996); A. Rahmani and F. de Fornel *Opt. Commun.* **131**, 253 (1996); S. K. Sekatskii and V. S. Letokhov, *Appl. Phys. B* **63**,

- 525 (1996); T. Pagnot, D. Barchiesi, D. Van Labeke, and C. Pieralli, *Opt. Lett.* **1501**, 120 (1997).
- [6] G. S. Agarwal, *Phys. Rev. A* **11**, 230 (1975); **11**, 243 (1975); **12**, 1475 (1975).
- [7] C. Girard, *Phys. Rev. B* **45**, 1800 (1992), *Pure Appl. Opt.* **1**, 157 (1992).
- [8] R. X. Bian, R. C. Dunn, X. S. Xie, and P. T. Leung, *Phys. Rev. Lett.* **75**, 4772 (1995).
- [9] T. V. Plakhotnik, *Opt. Spektrosk.* **79**, 747 (1995) [*Opt. Spectrosc.* **79**, 688 (1995)].
- [10] R. Chang, W. Fann, and S. H. Lin, *Appl. Phys. Lett.* **69**, 2338 (1996).
- [11] C. Girard, O. J. F. Martin, and A. Dereux, *Phys. Rev. Lett.* **75**, 3098 (1995); C. Girard and A. Dereux, *Rep. Prog. Phys.* **59**, 657 (1996).
- [12] L. Novotny, *Appl. Phys. Lett.* **69**, 3806 (1996).
- [13] M. Devel, C. Girard, and C. Joachim, *Phys. Rev. B* **53**, 13 159 (1996).
- [14] K. H. Drexhage, *J. Lumin.* **1,2**, 693 (1970); and in *Progress in Optics*, edited by E. Wolf (North-Holland, Amsterdam, 1974), Vol. XII, p. 165.
- [15] R. R. Chance, A. Prock, and R. Silbey, *J. Chem. Phys.* **60**, 2744 (1974).
- [16] R. E. Kunz and W. Lukosz, *J. Opt. Soc. Am.* **67**, 1607 (1977); **67**, 1615 (1977).
- [17] B. N. J. Persson and S. Anderson, *Phys. Rev. B* **29**, 4382 (1984).
- [18] J. M. Wylie and J. E. Sipe, *Phys. Rev. A* **30**, 1185 (1984); **32**, 2030 (1985).
- [19] J.-Y. Courtois, J.-M. Courty, and J. C. Mertz, *Phys. Rev. A* **53**, 1862 (1996).
- [20] M. S. Yeung and T. K. Gustafson, *Phys. Rev. A* **54**, 5227 (1996).
- [21] L. Novotny, *J. Opt. Soc. Am. A* **14**, 91 (1997); **14**, 105 (1997).
- [22] G. Barton, *Proc. R. Soc. London, Ser. A* **320**, 251 (1970).
- [23] M. R. Philpott, *Chem. Phys. Lett.* **19**, 435 (1973).
- [24] R. R. Chance, A. Prock, and R. Silbey, *Adv. Chem. Phys.* **37**, 1 (1978).
- [25] W. Lukosz, *Phys. Rev. B* **21**, 4814 (1980); **22**, 3030 (1980); *J. Opt. Soc. Am.* **71**, 744 (1981).
- [26] H. Nha and W. Jhe, *Phys. Rev. A* **54**, 3505 (1996).
- [27] S. Haroche in *Fundamental Systems in Quantum Optics*, edited by J. Dalibard, J. M. Raimond, and J. Zinn-Justin (North-Holland, Amsterdam, 1992), pp. 767–940.
- [28] J. Dalibard, J. Dupont-Roc, and C. Cohen-Tannoudji, *J. Phys. A* **43**, 1617 (1982); *J. Phys. (France)* **43**, 1617 (1982).
- [29] L. Landau and E. Lifchitz, *Physique Statistique* (Edition Mir, Moscow, 1967), Chap. 12.
- [30] I. S. Gradshteyn and I. M. Ryzhik, *Table of Integrals, Series and Products, Corrected and Enlarged Edition* (Academic, New York, 1980).
- [31] J. A. Stratton, *Electromagnetic Theory* (MacGraw-Hill, New York, 1941), Sec. 9.28.
- [32] *Handbook of Optical Constants of Solids*, edited by E. D. Palik (Academic, New York, 1985).
- [33] M. Moskovits, *Rev. Mod. Phys.* **57**, 783 (1985) and references therein; see also the references cited in Refs. [24] and [27].
- [34] W. Lukosz and R. E. Kunz, *Opt. Commun.* **20**, 195 (1977).
- [35] L. Schiff, *Quantum Mechanics*, 3rd ed. (McGraw-Hill, New York, 1968), pp. 414 and 532.
- [36] D. Meschede, W. Jhe, and E. A. Hinds, *Phys. Rev. A* **41**, 1587 (1990).
- [37] C. Girard, A. Dereux, and O. J. F. Martin, *Surf. Sci.* **295**, 445 (1993); C. Girard, X. Bouju, O. J. F. Martin, A. Dereux, C. Chavy, H. Tang, and C. Joachim, *Phys. Rev. B* **48**, 15 417 (1993); O. J. F. Martin, C. Girard, and A. Dereux, *Phys. Rev. Lett.* **74**, 526 (1995).
- [38] E. M. Purcell and C. R. Pennypacker, *Astrophys. J.* **186**, 705 (1973).
- [39] C. Girard, A. Dereux, O. J. F. Martin, and M. Devel, *Phys. Rev. B* **50**, 14 467 (1994).
- [40] V. V. Klimov and V. S. Letokhov, *Opt. Commun.* **122**, 155 (1996); *Phys. Rev. A* **54**, 4408 (1996).